Vol 16 No 10, October 2007
1009-1963/2007/16(10)/2998-06

Chinese Physics

© 2007 Chin. Phys. Soc.
and IOP Publishing Ltd

Analytic approach to the small-signal frequency response of saturated semiconductor optical amplifiers using multisection model*

Zhou En-Bo(周恩波), Zhang Xin-Liang(张新亮), and Huang De-Xiu(黄德修)

Wuhan National Laboratory for Optoelectronics, Huazhong University of Science and Technology, Wuhan 430074, *China*

(Received 9 January 2007; revised manuscript received 18 April 2007)

An analytic solution derived by multisection model to the small-signal frequency response (SSFR) of wavelength conversion based on cross-gain modulation (XGM) in semiconductor optical amplifiers (SOAs) is presented. The result contains details that can affect the characteristics of SSFR significantly more than previous ones.

Keywords: wavelength conversion, cross-gain modulation, frequency response, semiconductor optical amplifiers

PACC: 4265K, 4265G , 4280S

1. Introduction

Wavelength conversion in semiconductor optical amplifiers (SOAs) has been widely studied since the 1990s. Cross-gain modulation as a fundamental wavelength conversion principle has been applied to various optical communication systems and networks.[1−3] Small-signal frequency response (SSFR) as a modulation technology can be used for understanding device dynamic characteristics reflected by the key parameter of carrier lifetime. As systems operate at high speeds, the investigation of SSFR of SOA should consider more details as quantitatively as possible. Several papers have reported both theoretical analyses and numerical simulations in the last decade. Of them, two papers are the most important in the sense of both their analytic derivations and conclusions, in our opinion. One is Ref.[4], in which is developed an analytic solution of conversion efficiency showing that small-signal bandwidth of wavelength conversion also depends on the single-pass gain of the device. The conclusion drawn in the paper is further discussed in Ref.[5] in which is demonstrated a flaw in Davies's theory that the waveguide internal loss can strongly affect the converter performance when the spatial inhomogeneity is too intensive to be neglected. However the internal loss in Ref.[6] is still neglected due to the requirement for analytic solution to 3-dB frequency and optical modulation response. The quasi-analytic derivation from Ref.[7] demonstrates that the gain dispersion can also react on the frequency response. Numerical simulation is shown in Refs.[8] and [9] for a more accurate but less intuitional solution. It is worth mentioning that the transfer function introduced in Ref.[9] can give a better understanding of the resonance phenomena of SSFR for both co-propagation and counter-propagation schemes.

In this paper, we show a multisection approach to deriving the conversion efficiency. The results reveal that not only internal loss in waveguide but also geometrical parameters of device and current injection can affect the conversion efficiency, which cannot be directly indicated by the solution given by Mecozzi.[5]

2. Small signal analysis

For a harmoniously modulated pump signal and continuous probe wave incident upon the same facet of an SOA, the relevant small-signal equations are presented as

$$\frac{\partial N}{\partial t} = \frac{J}{eV} - R(N) - \sum_i (N - N_{t,i}) \frac{P_i}{E_{\mathrm{sat},i}}, \quad (1)$$

$$\frac{\partial P_i}{\partial z} = (\Gamma a_i (N - N_{t,i}) - \alpha_{\mathrm{int}}) P_i, \quad (2)$$

*Project supported by the National Nature Science Foundation of China (Grant No 60407001), National High Technology Developing Program of China (Grant No 2006AA03Z0414), the Science Fund for Distinguished Young Scholars of Hubei Province (Grant No 2006ABB017) and the Program for New Century Excellent Talents of Ministry of Education, China (Grant No NCET-04-0715).

where N is the carrier density along the cavity which is longitude-dependent. J is the SOA bias current. e is the elementary charge of electron. V is the active region volume. $E_{\mathrm{sat},i} = \dfrac{A\hbar\omega}{a_i\Gamma}$ is the saturation energy. P_i is the power of pump ($i = 1$) or continuous ($i = 2$) wave, $R(N)$ is the spontaneous recombination rate which is empirically demonstrated as $R(N) = AN + BN^2 + CN^3$, in which the three parameters A, B and C represent defect, radiative spontaneous and Auger recombination respectively. In the process of deviation, simple substitution of $R(N) = N/\tau_{\mathrm{s}}$ is adopted, which implies that the carrier lifetime is chosen to be independent of distribution of carrier concentrations along the SOA. $\tau_{\mathrm{s}} = [(\mathrm{d}R/\mathrm{d}N)|_{\bar{N}}]^{-1}$ is chosen to be a mean carrier density along the cavity, that means the density will be varied with different current injections, and a reasonable approximation may be taken into consideration.

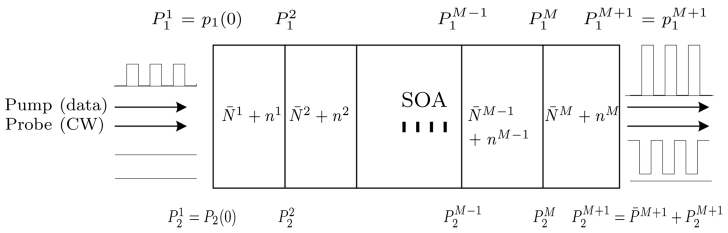


Fig.1. The multisection model for small-signal frequency response based on XGM principle. The powers of pump (dash) and probe (CW) beams and the carrier concentration are considered as constants within each section.

The carrier concentration along the SOA is divided into M sections in consideration of multisection approach (see Fig.1). For each section, the carrier concentration is harmoniously modulated as well as the probe wave, which can be separately treated as an average term and an oscillatory term, given by

$$N^k = \bar{N}^k + n^k \mathrm{e}^{-\mathrm{j}\omega t} + \mathrm{c.c}, \tag{3}$$

$$P_i^k = \bar{P}_i^k + p_i^k \mathrm{e}^{-\mathrm{j}\omega t} + \mathrm{c.c}, \tag{4}$$

where $k = 1, 2, \cdots, M$ each are section number. The average terms of $\bar{P}_i^k$ and $\bar{N}^k$ are considered as constants in each section. P_i^{M+1} is defined as the power of the output facet of the SOA. The input conditions can be written as $P_i^1 = P_i(0) + p_i(0)\,\mathrm{e}^{-\mathrm{j}\omega t}$. Inserting expressions (3) and (4) into Eqs.(1) and (2) one can obtain

$$\bar{N}^k = \frac{\frac{I}{eV} + \sum\limits_i \dfrac{N_{t,i}\bar{P}_i^k}{E_{\mathrm{sat},i}}}{1/\tau_{\mathrm{s}} + \sum\limits_i \dfrac{\bar{P}_i^k}{E_{\mathrm{sat},i}}}, \tag{5}$$

and

$$n^k = \sum_i X_i^k p_i^k, \tag{6}$$

where

$$X_i^k = -\frac{\dfrac{\left(\bar{N}^k - N_{t,i}\right)}{E_{\mathrm{sat},i}}}{1/\tau_{\mathrm{s}} + \sum\limits_i \dfrac{\bar{P}_i^k}{E_{\mathrm{sat},i}} - \mathrm{j}\omega}, \tag{7}$$

the powers of propagating lights

$$\bar{P}_i^{k+1} = G_i^k \bar{P}_i^k, \tag{8}$$

$$p_i^{k+1} = G_i^k \left(p_i^k + \Gamma a_i n^k \bar{P}_i^k l\right), \tag{9}$$

with l being the length of each section, defined as $l = \dfrac{L}{M}$. Expression (9) is microscopic when M is large enough. G_i^k is the saturated gain of pump ($i = 1$) or continuous ($i = 2$) wave in section k, defined as $G_i^k = \exp\left[\left(\Gamma a_i\left(\bar{N}^k - N_{t,i}\right) - \alpha_{\mathrm{int}}\right) l\right]$. Inserting expressions (5)–(7) into expressions (8) and (9) yields

$$\begin{aligned} & p_1^{k+1} - G_1^k\left(1 + \Gamma a_1 X_1^k \bar{P}_1^k l\right) p_1^k \\ &= G_1^k \Gamma a_1 X_2^k p_2^k \bar{P}_1^k l, \end{aligned} \tag{10}$$

$$\begin{aligned} & p_2^{k+1} - G_2^k\left(1 + \Gamma a_2 X_2^k \bar{P}_2^k l\right) p_2^k \\ &= G_2^k \Gamma a_2 X_1^k p_1^k \bar{P}_2^k l, \\ & k = 1, 2, \cdots, M. \end{aligned} \tag{11}$$

Expressions (10) and (11) including $2M$ equations are two very important recursive relationships between pump and probe lights mutually modulated. Two approximations are taken as $\bar{P}_1(0) \to 0$ and $p_2(0) \to 0$ from the general XGM principle as well as Ref.[4]. Applying these two approximations to expressions (8)–(11) yields

$$p_1^k = \left(\prod_m^{k-1} G_1^m\right) p_1(0), \tag{12}$$

$$p_2^{k+1} - G_2^k\left(1 + \Gamma a_2 X_2^k \bar{P}_2^k l\right) p_2^k = G_2^k \Gamma a_2 X_1^k \bar{P}_2^k l \left(\prod_m^{k-1} G_1^m\right) p_1. \tag{13}$$

Ordering $G_1^0 \equiv 1$, expression (13) can be written in the iterative form

$$p_2^{k+1} = p_1^1 \sum_{i=1}^{k} \left[\left(\prod_{m=i}^{k} G_2^m\left(1 + \Gamma a_2 X_2^m \bar{P}_2^m l\right)\right) \frac{\Gamma a_2 X_1^i \bar{P}_2^i l}{1 + \Gamma a_2 X_2^i \bar{P}_2^i l} \left(\prod_{m=0}^{i-1} G_1^m\right)\right], \tag{14}$$

while ordering $\prod_{m=k+1}^{k}\left(1 + \Gamma a_2 X_2^m \bar{P}_2^m l\right) \equiv 1$, the conversion efficiency can be written as

$$T^{k+1} = \left|\frac{p_2^{k+1}}{p_1^1}\right| = \left|\sum_{i=1}^{k}\left\{\prod_{m=i}^{k} G_2^m \prod_{m=0}^{i-1} G_1^m \prod_{m=i+1}^{k}\left[\left(1 + \Gamma a_2 X_2^m \bar{P}_2^m l\right)\right] \Gamma a_2 X_1^i \bar{P}_2^i l\right\}\right|. \tag{15}$$

Expression (15) is an accurate solution for a probe wave carrying the inverted signal of pump light. However, expression (15) is extremely complex so that only numerical solution can reveal its implication. In order to better understand it, a few approximations must be taken as below. Assuming there exists a slightly frequency deviation between the two waves (but the detuning between the two fields is large than the inverse stimulated carrier lifetime divided by 2π, as a result, the four-wave mixing effects can be neglected). Assuming $a_1 = a_2 = a$ leads to $G_1^k = G_2^k = G^k$, $E_{\text{sat},1} = E_{\text{sat},2} = E_{\text{sat}}$, $N_{t,1} = N_{t,2} = N_t$ and $X_1^k = X_2^k = X^k$, which are easily elicited. Applying these simplifications to expression (15), we can rewrite the conversion efficiency as

$$T^{k+1} = \left|G_{\text{s}}^k\left\{\prod_{m=1}^{k}\left[\left(1 + \Gamma a X^m \bar{P}_2^m l\right)\right] - 1\right\}\right| = \left|G_{\text{s}}^k\left\{\exp\left(\int_0^{kl} \Gamma a X \bar{P}_2 \mathrm{d}z\right) - 1\right\}\right| \tag{16}$$

$$= \left|G_{\text{s}}^k\left\{\exp\left[\frac{C}{C-\omega}\left(\ln\left(1 - \frac{(G^k-1)P_2(0)/E_{\text{sat}}}{1/\tau_{\text{s}} + G^k P_2(0)/E_{\text{sat}} - \mathrm{j}\omega}\right) - \ln\left(\frac{1 - \frac{1}{C}(1/\tau_{\text{s}} + P_2(0)/E_{\text{sat}})}{1 - \frac{1}{C}(1/\tau_{\text{s}} + G^k P_2(0)/E_{\text{sat}})}\right)\right)\right] - 1\right\}\right|, \tag{17}$$

where

$$G_{\text{s}}^k = \prod_{m=1}^{k} G^m, \tag{18}$$

$$C = \left(\frac{I}{eV} - \frac{N_t}{\tau_{\text{s}}}\right)\frac{\Gamma a}{\alpha_{\text{int}}}. \tag{19}$$

Rewriting G_{s}^M as G_{s} which is defined as the single pass gain of the amplifier, one can obtain

$$\ln(G_{\text{s}}) = \Gamma a l \sum_{\text{k}=1}^{M}\left(\bar{N}^k - N_t\right) - \alpha_{\text{int}} L = C\int_{P_2(0)}^{P_2(L)} \frac{1}{P_2}\frac{1}{C - \left(\frac{1}{\tau_{\text{s}}} + \frac{P_2}{E_{\text{sat}}}\right)}\mathrm{d}P_2 - \alpha_{\text{int}} L$$

$$= \frac{C}{C - 1/\tau_{\text{s}}}\left(\ln(G_{\text{s}}) - \ln\frac{C - \left(\frac{1}{\tau_{\text{s}}} + \frac{G_{\text{s}}P_2(0)}{E_{\text{sat}}}\right)}{C - \left(\frac{1}{\tau_{\text{s}}} + \frac{P_2(0)}{E_{\text{sat}}}\right)}\right) - \alpha_{\text{int}} L. \tag{20}$$

From expression (17), we can write the final expression of the conversion efficiency defined as the ratio between the powers of the oscillation terms of output probe and input pump lights as

$$T(\omega) = \left|G_{\text{s}}\left\{\exp\left[\frac{C}{C - \mathrm{j}\omega}\left(\ln\left(1 - \frac{(G_{\text{s}}-1)P_2(0)/E_{\text{sat}}}{1/\tau_{\text{s}} + G_{\text{s}}P_2(0)/E_{\text{sat}} - \mathrm{J}\omega}\right) - \ln\left(\frac{1 - \frac{1}{C}(1/\tau_{\text{s}} + P_2(0)/E_{\text{sat}})}{1 - \frac{1}{C}(1/\tau_{\text{s}} + G_{\text{s}}P_2(0)/E_{\text{sat}})}\right)\right)\right] - 1\right\}\right|. \tag{21}$$

Expressions (20) and (21) are the main results of this paper. Equation (20) can be easily solved for G_s by using the boundary condition of input power $P_2(0)$. Notice that, the conversion efficiency in expression (21) can be affected by the parameter of C defined in expression (19) consisting of geometric parameters of the SOA, current injection and waveguide internal loss.

3. Result and discussion

The conversion frequency in expression (21) is compared with the results of inclusion gain dispersion to evaluate the deviation from the numerical simulation as shown in Figs.2 and 3. The amplified spontaneous emission (ASE) noise is neglected for the simplification of numerical simulation. Also, the spontaneous recombination rate is expressed as a cubic polynomial. The differential gain coefficient and the transparent carrier density for different wavelengths of beams are calculated from Ref.[10], which can be also measured experimentally. Figures 2 and 3 show the SSFR in short ($500\,\mu m$) and long ($1500\,\mu m$) SOAs biased at 120 mA and 360 mA, respectively. In Figs.2 and 3, the solid line and dash line are for our analytic solution and numerical simulation, respectively. The symbols of cross and triangle represent downconversion and upconversion schemes where the wavelengths of two channels are chosen to be 1540 nm and 1550 nm respectively. The internal loss is set to be $10000\,\mathrm{m}^{-1}$ and the other parameters are listed in Table 1 for both SOAs.

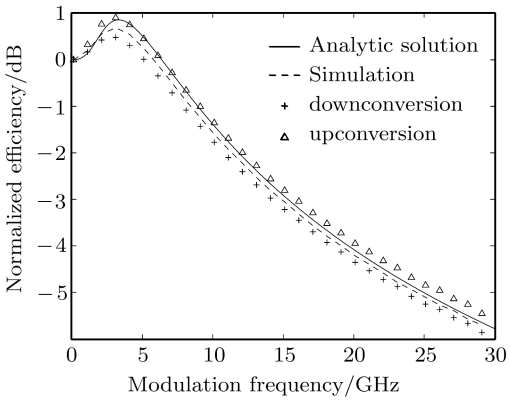


Fig.2. Comparison of normalized conversion efficiency among analytic solution (solid), simulation without gain dispersion (dash), simulation of downconversion (cross) and upconversion (triangle). The SOA is biased at 120mA and the length is set to be $500\,\mu$m.

In Fig.2, the three simulation curves (downconversion, upconversion and without gain dispersion) are quite close to our analytic solution. The most prominent deviation between our analytic solution and simulation without gain dispersion occurs near the resonance peak, and it is no more than 5% in value. That is due to the approximation of spontaneous recombination rate in our approach. With the inclusion of gain dispersion the SSFRs of downconversion and upconversion differ little from our result, which is due to the fact that the disparity in gain between the two beams is reduced by the short length of the unsaturated device.

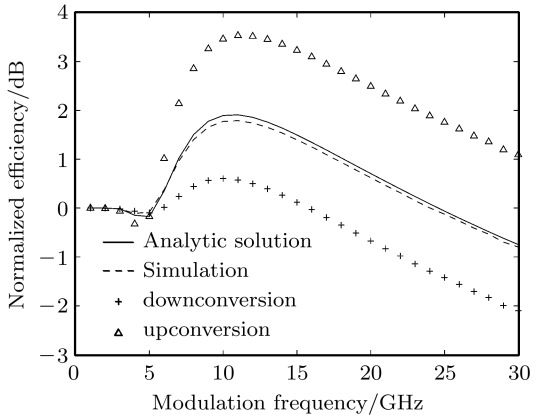


Fig.3. Comparison of normalized conversion efficiency among analytic solution (solid), simulation without gain dispersion (dash), simulation of downconversion (cross) and upconversion (triangle). The SOA is biased at 360mA and the length is set to $1500\,\mu$m.

In Fig.3, the simulation result without gain dispersion is quite similar to the analytic one. However, the SSFRs of downconversion and upconversion have a significant difference from ours. This is because the device is long enough to amplify two waves thoroughly, causing deep saturation in the end of the device and bringing a different gain to the two fields.

In Eq.(16), when ordering $M = 1$ and $g = \Gamma a\left(\bar{N} - N_t\right)$, one can obtain the result in Ref.[4] quickly, although the definition of conversion efficiency in Ref.[4] differs from ours by a factor of single pass gain. Obviously, for that approximation, the integration is based on the homogeneous distributions of carrier concentrations and light powers. Also the infinitesimal term in derivation is too large to be neglected. As a result, the characteristic of the conversion efficiency is incomplete.

If we order $C = 1/\left(\tau_s \xi\right)$ and $E_{sat}/\tau_s = P_{sat}$ in expressions (20) and (21), we may obtain the results in Ref.[5] differing by a gain factor due to different definition of efficiency.

Table 1. Symbols and values in calculation.

Parameter	symbol	Value
Active region thickness	d/μm	0.2
Active region width	w/μm	1.5
Transparency carrier density	N_t/m^{-3}	1.16×10^{24}
Differential gain coefficient	a/m^2	7.91×10^{-20}
Optical confinement factor	Γ	0.45
Defect recombination coefficient	A/s^{-1}	3.6×10^{8}
Spontaneous recombination coefficient	$B/\mathrm{m}^3\mathrm{s}^{-1}$	5.6×10^{-16}
Auger recombination coefficient	$C/\mathrm{m}^6\mathrm{s}^{-1}$	3.0×10^{-41}

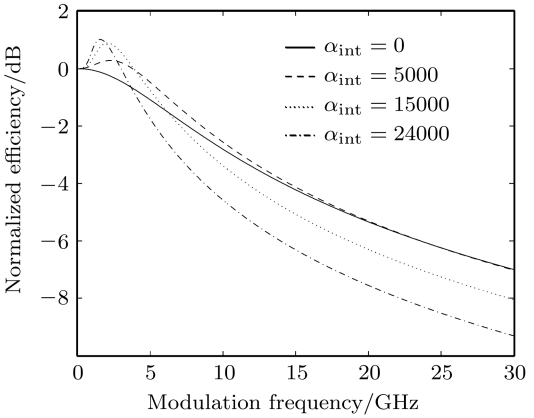


Fig.4. Conversion efficiency versus modulation frequency for different waveguide internal losses.

Figure 4 shows the normalized efficiency versus the modulation frequency for different values of internal loss. The SOA is biased at 120 mA, the length of active region is 500 μm, and the other parameters are listed in Table I. The solid line in Fig.4 is for a lossless (ideal) SOA that reflects the low-pass characteristics as reported before. The dash line is for $\alpha_{\mathrm{int}} = 5000\,\mathrm{m}^{-1}$ corresponding to the normalized loss of 0.1 treated in Ref.[5]. A slight resonance phenomenon is manifested. The dotted and dash-dotted lines are for $\alpha_{\mathrm{int}} = 15000\,\mathrm{m}^{-1}$ and $\alpha_{\mathrm{int}} = 24000\,\mathrm{m}^{-1}$, corresponding to the normalized losses of 0.3 and 0.5 respectively. The resonance peak is quite prominent especially for larger values of internal loss, however, which are unrealistic for a normal SOA.

The normalized efficiency versus modulation frequency for different values of injection current is shown in Fig.5 corresponding to $\alpha_{\mathrm{int}} = 10000\,\mathrm{m}^{-1}$. The resonance peak shifts toward high frequencies with the bias current increasing monotonically. Consequently, the 3-db band width has also increased for high injection levels which can be easily understood.

Figure 6 is SSFR for different lengths of SOAs under the condition of $I = 120\,\mathrm{mA}$ and $\alpha_{\mathrm{int}} = 10000\,\mathrm{m}^{-1}$, which manifest an analogical characteristic for different injection currents.

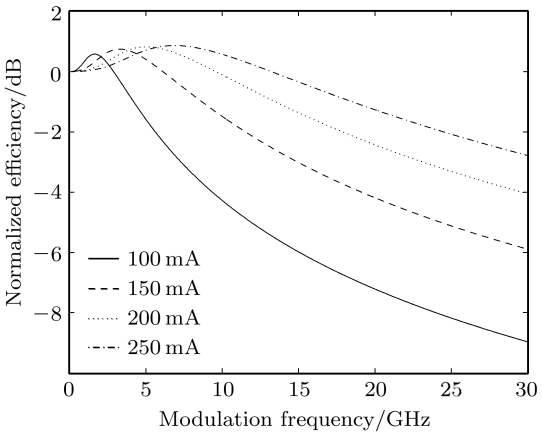


Fig.5. Conversion efficiency versus modulation frequency for different bias currents.

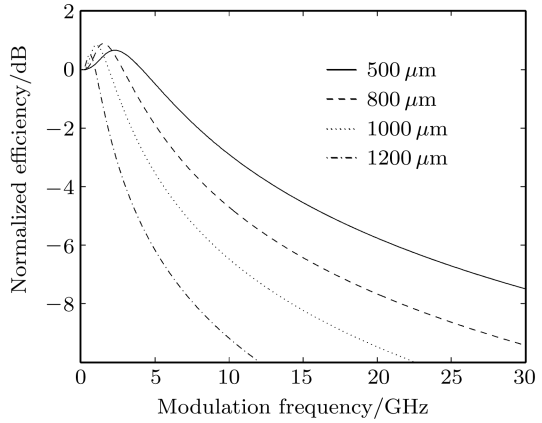


Fig.6. Conversion efficiency versus modulation frequency for different waveguide lengths.

4. Conclusion

A new analytic approach to demonstrating the SSFR of wavelength conversion based on cross-gain modulation (XGM) in semiconductor optical amplifiers (SOAs) is presented.The results uncover the internal relationship between characteristics of SSFR and waveguide internal loss, device geometrical parameters as well as current injection. Also, the results manifest that gain dispersion affects the SSFR more prominent in long SOAs than short ones as a result of deeper saturation in the former.

References

[1] Dong J J and Zhang X L 2007 *Chin. Phys.* **16** 2250
[2] Li P L, Zhang X L, Huang D X and Zhu G X 2006 *Chin. Phys.* **15** 2746
[3] Wang Y, Zhang X L and Huang D X 2004 *Chin. Phys.* **13** 882
[4] Davies D A O 1995 *IEEE Photon. Technol. Lett.* **7** 617
[5] Mecozzi A 1996 *IEEE Photon. Technol. Lett.* **8** 1471
[6] Marcenac D and Mecozzi A 1997 *IEEE Photon. Technol. Lett.* **9** 749
[7] Sun J Q, Huang D X and Yi H Q 1997 *Chin. Phys.* **6** 2369
[8] Obermann K, Kindt S, Breuer D and Petermann K 1998 *J. Lightwave Technol.* **16** 78
[9] Nielsen M L, Blumenthal D J and Mork J 2000 *J. Lightwave Technol.* **18** 2151
[10] Connelly M J 2001 *IEEE J. Quantum Electron.* **37** 439